

Rigidity of disordered networks with bond-bending forces

Michael Plischke

Physics Department, Simon Fraser University, Burnaby, British Columbia, Canada V5A 1S6

(Received 24 November 2006; revised manuscript received 8 May 2007; published 13 August 2007)

At zero temperature, the elastic constants of a disordered network with bond-bending forces vanish at the geometric percolation point p_c , in contrast to networks with only central forces which lose the ability to withstand shear at a rigidity percolation point p_r . Moreover, the critical behavior of the modulus is different in the two cases. I report on extensive molecular dynamics simulations on a model system with central and bond-bending forces between the monomers over a range of temperatures T . The critical behavior of the shear modulus seems to be the same as that of a purely central-force network at finite T and consistent with a long-standing conjecture of de Gennes.

DOI: [10.1103/PhysRevE.76.021401](https://doi.org/10.1103/PhysRevE.76.021401)

PACS number(s): 82.70.Gg, 61.43.-j, 62.20.Dc

I. INTRODUCTION

Since the initial observation by Feng and Sen [1] that the elastic constants (at $T=0$) of a disordered central-force network vanish at a concentration of sites or bonds, p_r , that generically is different from the geometric percolation concentration p_c , there has been a great deal of discussion of this problem, as well as some controversy. Predating the work of [1] is a prediction of de Gennes [2] that the critical behavior of the elasticity of disordered networks should be the same as that of the conductivity of a disordered network of resistors. Since the conductivity of the resistor network remains finite for all $p > p_c$, this prediction clearly is not valid at $T=0$. Subsequently, Kantor and Webman [3] pointed out that if bond-bending forces between particles are included, $p_r=p_c$. However, in both two and three dimensions the critical behavior of the moduli, at $T=0$, is very different from that of the conductivity of the disordered resistor network [4] for both the central-force and bond-bending cases [5,6].

Several years ago, we began a study of disordered central-force networks at finite temperature [7,8]. Generically, these networks have an entropy-generated component in their moduli that remains finite for all $p > p_c$. Moreover, in both two and three dimensions the critical behavior of the shear modulus is consistent with the de Gennes prediction. More recent work [9–11] has provided additional support for this conclusion for a variety of different microscopic models with central forces. In the language of the renormalization group, these simulations suggest that temperature is a relevant variable that generates a flow from the zero-temperature fixed point at p_r to a finite-temperature Gaussian fixed point on the line $p=p_c$. It should, however, be noted that a recent renormalization group calculation [12] has arrived at the conclusion that the Gaussian fixed point is itself unstable although there are some indications [11] that the model used by these authors may not be complete.

In this article, I report on molecular dynamics (MD) simulations for a model that includes central and bond-bending forces in two and three dimensions. In both cases, the results are consistent with a crossover from zero-temperature critical behavior to a finite-temperature fixed point. The critical exponent t that describes the asymptotic behavior of the modulus is, in both cases, consistent with the random resistor analogy.

The structure of this article is as follows. In the next section (Sec. II) I describe the model used and give some of the computational details. Section III contains the results in the two-dimensional case and the three-dimensional results are discussed in Sec. IV. I conclude with a short summary in Sec. V.

II. MODEL

I consider systems of size L^2 with $L \leq 96$ particles in $d=2$ and size L^3 with $L \leq 32$ in $d=3$. The particles are initially placed on the vertices of a square (simple cubic) lattice and are tethered to each other by a nearest-neighbor potential of the form $V(r) = \frac{1}{2}k(r-r_0)^2$. The lattice spacing is taken to be $r_0=1$ so that the system is not under energetic tension. A fraction p of these nearest-neighbor bonds is retained. This corresponds to bond percolation for which $p_c(d=2)=0.5$ and $p_c(d=3) \approx 0.2488$. Once this process is completed, the spanning cluster, if one exists, is identified and the remaining finite clusters are discarded. To this point, the model is identical to that studied in [7,8]. In more recent work [11] I have presented evidence that the addition of excluded-volume interactions does not affect the critical behavior of the shear modulus and, for computational efficiency, I have neglected these in the present case. Bond-bending forces are conveniently introduced in the following way. For three nearest neighbors i , j , and k with nearest-neighbor bonds meeting at a right angle in the initial on-lattice configuration, I add the three-particle potential

$$V_{bb}(\mathbf{r}_i, \mathbf{r}_j, \mathbf{r}_k) = \frac{1}{2}v_{ang}[\hat{\mathbf{n}}_{ij} \cdot \hat{\mathbf{n}}_{ik}]^2, \quad (1)$$

where, e.g., $\hat{\mathbf{n}}_{ij}$ is the unit vector from particle i to particle j and particle i is at the vertex of the right angle. This potential, as long as $k_B T \ll v_{ang}$, will allow only small deviations from the original right angle configurations. For a triplet of particles with collinear nearest-neighbor bonds, the same form of potential with a minus sign in front of v_{ang} is used.

Once the system has been diluted and the particles interacting through three-body forces identified, the system is equilibrated using periodic boundary conditions and a velocity-Verlet Brownian dynamics algorithm [13] to inte-

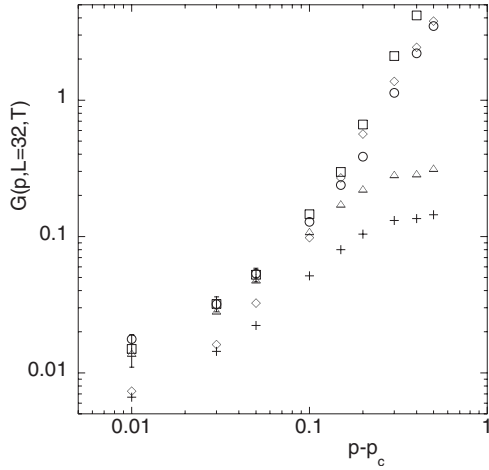


FIG. 1. Comparison of the shear modulus for the two cases $v_{ang}=0$ and $v_{ang}=1.0$ for $L=32$ and $T=0.25$ and $T=0.1$. For all p shown, $G \propto T$ in the central-force case (crosses and triangles), indicating entropic dominance, whereas energy dominates in the bond-bending case (circles and diamonds) for $p \geq 0.7$. Also shown (squares) is $G(p, T=0.25, v_{ang}=2.0)$. For the three smallest values of p , I have included error bars. For the remaining points the error bars are smaller than the symbols.

grate the equations of motion [14]. I take $k=5.0$ and, for most of the calculations, $v_{ang}=1.0$ and use a time step that is temperature dependent: $\delta t = 0.005 \sqrt{m r_0^2 / k_B T}$ for temperatures in the range $k_B T / v_{ang} = 0.005 - 1.0$. The system is typically equilibrated for $10^5 L^2$ time steps. The components of the stress tensor $\sigma_{\alpha\beta}$ are obtained from a virial equation, first for an undistorted computational box and then, after reequilibration, for a box that has been sheared by an amount γ . Reequilibration is necessary because all particles are initially displaced affinely—i.e., $x_i \rightarrow x_i + \gamma y_i$. The shear modulus is then obtained from

$$G(p, T, L) = -f_{perc}(p, L) \langle [\sigma_{xy}(\gamma) - \sigma_{xy}(0)] / \gamma \rangle, \quad (2)$$

where $f_{perc}(p, L)$ is the fraction of samples of size L that percolate at probability p and where the angular brackets denote an average over different realizations of the cross-links. All results displayed here are obtained using $\gamma=0.05$. This value of γ is small enough to ensure that the response is in the linear regime but still large enough to make the two values of the stress tensor measurably different. The number of different realizations of the cross-links varies with p but for all L and $\epsilon = p - p_c \leq 0.1$ is not less than 1000 and, in most cases, is much larger than that. Such large numbers of samples are necessary because the sample-to-sample variation of the modulus is large for $\epsilon < 0.1$.

III. TWO DIMENSIONS

I begin by comparing the behavior of the shear modulus for systems with and without angular forces. In Fig. 1, I plot the shear modulus for a system of linear dimension $L=32$ for $v_{ang}=0$ and $v_{ang}=1.0$ and temperatures $T=0.25$ and 0.1 as function of $p - p_c$. For the central force network, the values

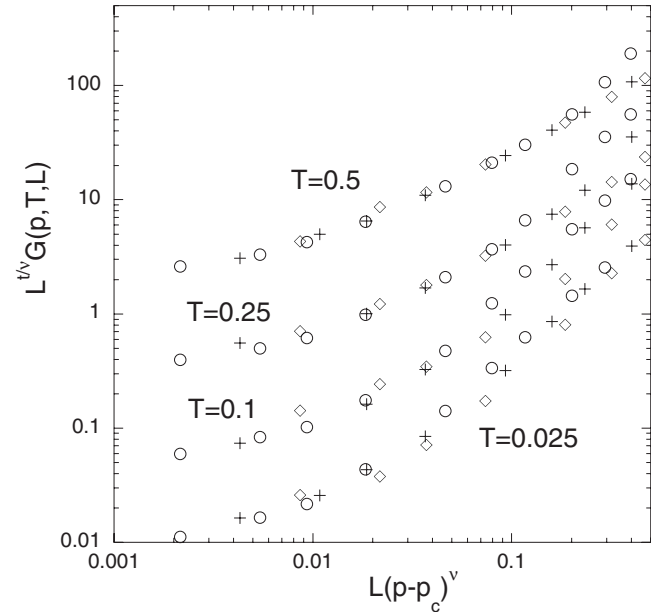


FIG. 2. Finite-size scaling plot of the dimensionless shear modulus for several values of T (in units of v_{ang}/k_B) for $L=16, 32$, and 64 . The value of the exponent $\nu = \frac{4}{3}$ and t is a temperature-dependent effective exponent (see the text). Circles, $L=16$; crosses, $L=32$; diamonds, $L=64$.

of $G(p, T=0.25)$ are almost exactly 2.5 as large as those of $G(p, T=0.1)$, for all values of p , demonstrating the primary role of entropy over the entire range of p . By contrast, for $v_{ang}=1.0$, there is a relatively weak temperature dependence for $p \geq 0.6$. Below that value of p , the bond-bending network also has its elasticity predominantly determined by entropy and the values of $G(p, T, v_{ang}=1.0)$ merge with those of the central-force network. This is already an indicator that the finite-temperature critical exponent for the bond-bending network is likely to be the same as that of the central-force network. Also shown is the modulus for $T=0.25$ and $v_{ang}=2.0$. This also becomes entropy dominated but at a somewhat lower value of $p - p_c$.

I next display the behavior of the shear modulus of the bond-bending model for several values of T as function of p . In the case of a state function that, in the thermodynamic limit, takes the form $G(p \rightarrow p_c, L = \infty) \sim (p - p_c)^t = \epsilon^t$ one expects the finite-size scaling form

$$G(p, L) = L^{-t\nu} \Phi(L/\xi(p)), \quad (3)$$

where $\xi(p) \sim \epsilon^{-\nu}$ is the relevant correlation length. Moreover, the scaling function $\Phi(x) \rightarrow \text{const}$ as $x \rightarrow 0$ and $\Phi(x) \sim x^{t\nu}$ for $L \gg \xi$. In our case, we have an added complication: the temperature may be a relevant variable; i.e., the value of the exponent t may be different for $T=0$ than for finite T . Therefore, I have used an effective exponent $t_{eff}(T)$ to obtain the best collapse of the data at a given temperature. Figure 2 shows $L^{t_{eff}\nu} G(p, T, L)$ as function of $L(p - p_c)^\nu$ for $k_B T / v_{ang} = 0.025, 0.1, 0.25$, and 0.5 for $L=16, 32$, and 64 , where $\nu = \frac{4}{3}$ is the known percolation correlation length exponent. The values of the effective exponent are $t_{eff}(0.025) = 1.93$,

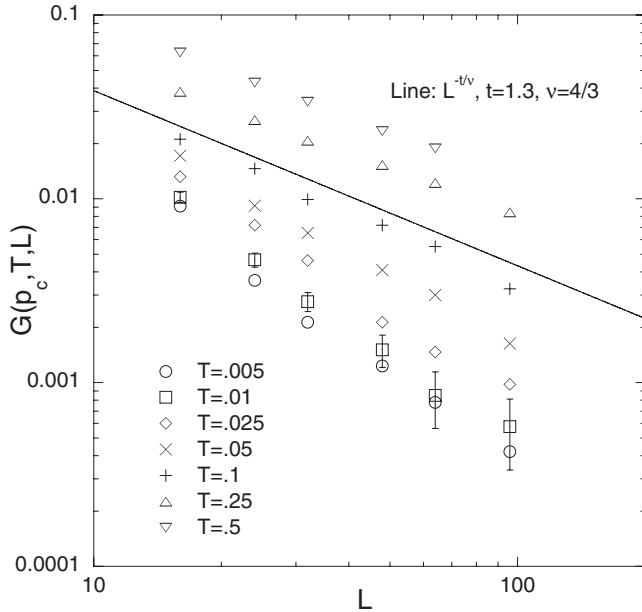


FIG. 3. The dimensionless shear modulus at $p=p_c$ for $0.005 \leq T \leq 0.5$ plotted as function of L for $16 \leq L \leq 96$. If $G(p, T, \infty) \sim (p-p_c)^t$ then we expect that $G(p_c, T, L) \sim L^{-t/\nu}$ where $\nu = \frac{4}{3}$ is the geometric percolation correlation length exponent. The solid line shows this function for $t=1.3$.

$t_{eff}(0.1)=1.77$, and $t_{eff}(0.25)=t_{eff}(0.5)=1.30$. The last two are consistent with the best estimates of the critical exponent of the shear modulus in central-force networks at nonzero temperature as well as with the prediction of de Gennes. This suggests that at finite temperature (in the thermodynamic limit $L \rightarrow \infty$) there is only one type of critical behavior, independent of whether or not bond-bending forces are present.

Further information can be obtained from a study of the modulus at $p=p_c$ as a function of L and T . At p_c the probability that a system of a given size L percolates is independent of L and the modulus is expected to scale as $G(p_c, T, L) \sim L^{-t/\nu}$ as is clear from Eq. (3) and the subsequent discussion. In Fig. 3, we show the raw data for the modulus for a range of temperatures as function of L . When the individual data sets are fit to a power law, two features are evident: (i) At the lowest temperatures, a pure power law does not provide a very good fit to the data and (ii) the curvature is such that an effective L -dependent exponent at fixed T tends toward smaller values as L becomes larger. This is in contrast to a similar plot, using data from Zabolitzky *et al.* [5] for the two-dimensional honeycomb lattice at $T=0$, for which the effective exponent *increases* as function of L . The straight line in the figure represents the anticipated power law with $t=1.30$ and, already for $T=0.1$, the last four data points are entirely consistent with this choice of t .

It is possible to combine all these data into a single universal curve. Since one expects that at $T=0$, $G(p_c, 0, L) \sim L^{-t(T=0)/\nu}$, with $t(T=0)$ the rigidity percolation exponent $t(T=0) \approx 3\nu$ [5], I plot, in Fig. 4, $\tilde{G} \equiv L^3 G(p_c, T, L)$ as function of $x = TL^\phi$. Varying ϕ , I find a respectable collapse of the data for $\phi = 2.9 \pm 0.3$ and this is illustrated for $\phi = 2.9$ in Fig. 4. We see (the inset) that at small values of x the data tend to

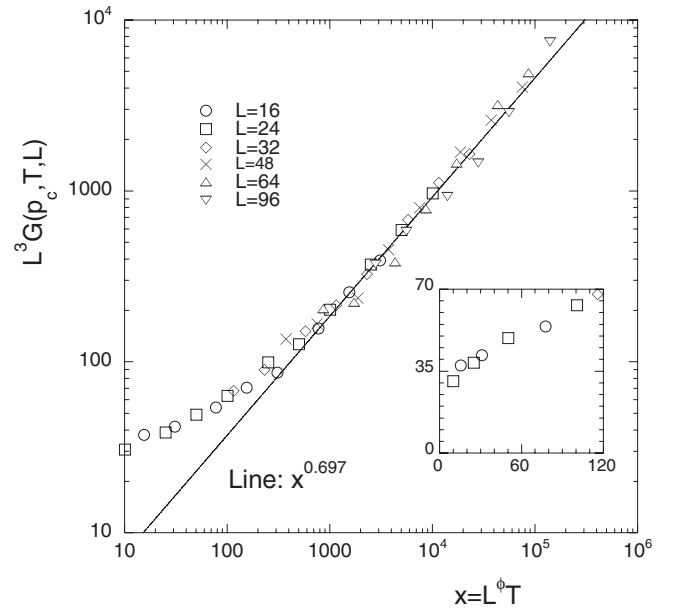


FIG. 4. The data of Fig. 3 replotted in a finite-size scaling form. For $t=1.3$ the expected behavior for $x \gg 1$ is $x^{0.697}$ where $x = L^\phi T$ with $\phi = 2.9$. The inset shows the low- x part of the data on a linear scale. This clearly indicates a finite limit at $x=0$ which is consistent with the conclusion of [5] that $t(T=0)/\nu \approx 3$.

a constant, consistent with the expected zero-temperature behavior. If the finite-temperature critical exponent is $t \approx 1.30$, then we should see a range of x over which $\tilde{G} \sim x^\lambda$ with $\lambda \approx 0.697$ since we expect the L dependence of $G(p_c, T, L)$ to be $L^{-t/\nu}$, leading to $\lambda = (3-t/\nu)/\phi \approx 0.697$. This behavior is given by the straight line in the figure, and we see that the data track this curve quite closely over more than two decades in x .

I also note that this value of ϕ implies a nontrivial temperature dependence for $G(p_c, T, L = \infty) \sim T^\lambda$ near the zero-temperature fixed point. For any finite L this behavior is masked by the fact that $\lim_{T \rightarrow 0} G(p_c, T, L) \neq 0$. Therefore, in Fig. 5, I display a fit of the data, for a few values of L , to the function $a(L) + b(L)T^\lambda$ for $\lambda = 0.697$. While not spectacular, the fit is reasonably good, lending support to the foregoing discussion. If confirmed by more extensive simulations, this would indicate that the zero-temperature fixed point for the bond-bending model is a multicritical point with at least two relevant variables. This is consistent with our picture of the rigidity percolation fixed point for systems with only central forces which is also unstable with respect to T and for which, at least for particles with hard cores, there are indications [11] that there are two independent diverging correlation lengths.

IV. THREE DIMENSIONS

In three dimensions, the best available estimate for t is [6] $t(T=0) = 3.78 \pm 0.09$ which results in $t(T=0)/\nu \approx 4.3$ which is very much larger than the de Gennes conjecture $t/\nu \approx 2.27$. It is therefore likely that even the small systems that I am able

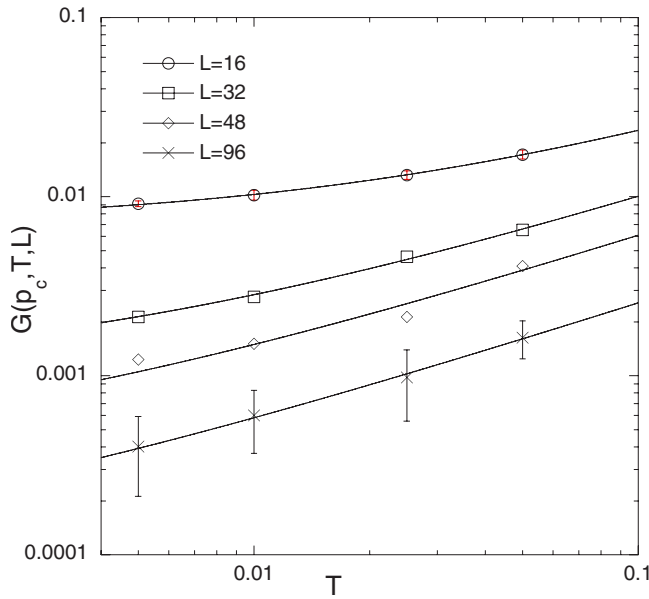


FIG. 5. (Color online) The function $G(p_c, T, L)$ plotted as a function of T at fixed L . The lines are fits to the function $a(L) + b(L)T^\lambda$ with $\lambda=0.697$ (see text).

to simulate in three dimensions can distinguish between these alternatives. I begin by displaying $G(p, T, L)$ as a function of p for $T=0.25$ and $T=0.5$ for $L=5, 8,$ and 12 for the first case and $L \leq 20$ for $T=0.5$. The raw data (Fig. 6) show the usual finite-size effects near p_c . The temperatures used here are high enough that the crossover seen in two dimensions seems to be complete because we obtain a very satisfactory collapse of the data (Fig. 7) for $t(0.25)=t(0.5)=2.0 \pm 0.2$, the value predicted by the random resistor analogy.

Figure 8 shows the data for $G(p=0.2488, T, L)$ as function of L for $0.025 \leq T \leq 0.5$ together with the line $L^{-t/\nu}$ with $t=2.0$ and $\nu=0.88$. On this graph, the crossover from $T=0$ behavior to the finite-temperature behavior is barely visible at even the lowest temperature. This implies that in an analo-

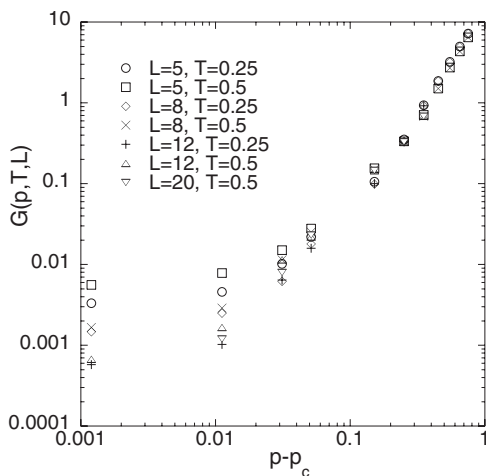


FIG. 6. The modulus $G(p, T, L)$ in three dimensions as function of p for several values of L for $T=0.25$ and 0.5 .

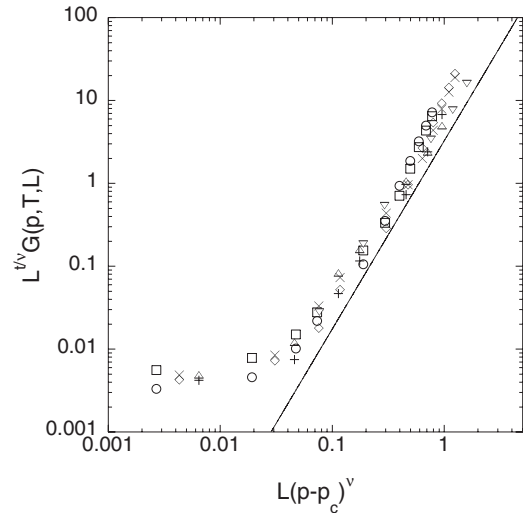


FIG. 7. The data of Fig. 6 replotted in finite-size scaling form using $t=2.0$ and $\nu=0.88$.

gous plot to Fig. 4 the crossover to the zero-temperature behavior will be less pronounced and, perhaps, invisible. This is indeed the case. As in two dimensions, the data of Fig. 8 can be collapsed quite well to a universal curve by plotting $L^{t(T=0)/\nu} G(p_c, T, L)$ as function of $x=L^{\phi} T$ with $\phi=2.8 \pm 0.4$ where the error is determined visually. At the outer limits of ϕ , the dispersion of the data is clearly greater than the statistical error in individual values of G . I note that the value $t(T=0)/\nu \approx 4.5$ or $t(T=0)=3.96$ is outside the maximum value allowed by the error bar on the exponent $t(T=0)$ [6]. It is well known that to obtain reliable values of this exponent in both two and three dimensions [5,6] corrections to scaling must be taken into account. The present analysis does not account for such effects, and this may explain the discrepancy.

Recovery of the zero-temperature behavior requires the scaling function to approach a finite limit as $x \rightarrow 0$. It is not obvious from the range of data available that this is the case.

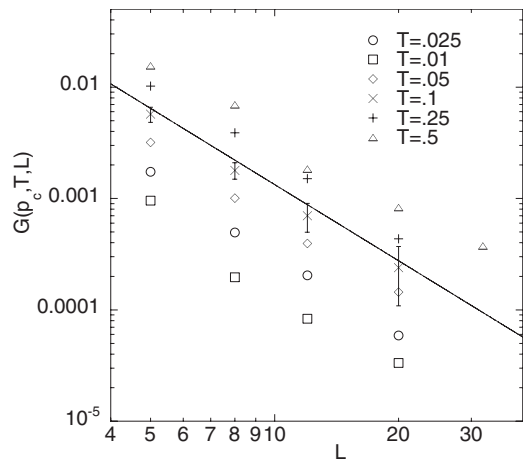


FIG. 8. $G(p \approx p_c, T, L)$ as a function of L for $0.005 \leq T \leq 0.5$. The solid line represents a power law $G \sim L^{-t/\nu}$ with $t=2.0$ and $\nu=0.88$.

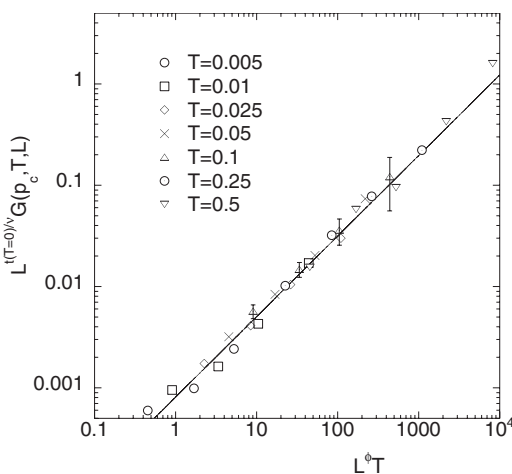


FIG. 9. The data of Fig. 8 replotted in finite-size scaling form. $L^{t(T=0)/\nu} G(p_c, T, L) = \Psi(TL^\phi)$ with $t(T=0) = 3.96$ and $\phi = 2.8$. If $t(T \neq 0) = 2.0$, then $\Psi(x) \sim x^\lambda$ with $\lambda = 0.795$ for $x \gg 1$. The solid line in the figure represents this behavior.

However, there are some encouraging signs of curvature at the smallest values of x .

V. CONCLUSION

The results presented here, together with previous work [7–11], suggest that for the class of models we have investi-

gated (central forces, with or without hard cores and central as well as three-body bond-bending forces) there is a single finite-temperature fixed point that describes the critical behavior of the modulus. It is located on the line $p = p_c$ and the flow from both the rigidity percolation fixed points ($T=0, p = p_r$) and ($T=0, p = p_c$) is toward this point. Moreover, all of our simulations indicate that the exponent t that describes the critical behavior of the modulus is, within numerical uncertainty, the same as the conductivity exponent in disordered resistor networks in both two and three dimensions. As well, the results presented here indicate that close to percolation the temperature dependence of the shear modulus is not linear in T (as one might expect because of its entropic origin) but rather $G(T, p \approx p_c) \sim T^\lambda$ with $\lambda(d=2) \approx 0.7$ and $\lambda(d=3) \approx 0.8$.

It must be acknowledged that neither the experimental situation nor the theoretical results are as unambiguous as my conclusions. There exists a body of experimental work [15] that supports the de Gennes conjecture but also work [16] that is consistent with a heuristic scaling argument [17] and a renormalization group calculation [12] that yield $t = d\nu$ where d is the dimensionality. As well some simulations of a lattice model also suggest this result [18].

ACKNOWLEDGMENTS

This research was supported by the NSERC of Canada. I thank Paul Goldbart, Xiangjun Xing, and Annette Zippelius for helpful discussions.

-
- [1] S. Feng and P. N. Sen, Phys. Rev. Lett. **52**, 216 (1984).
 [2] P.-G. de Gennes, J. Phys. (France) Lett. **37**, L1 (1976).
 [3] Y. Kantor and I. Webman, Phys. Rev. Lett. **52**, 1891 (1984).
 [4] S. Feng, P. N. Sen, B. I. Halperin, and C. J. Lobb, Phys. Rev. B **30**, 5386 (1984); S. Feng and M. Sahimi, *ibid.* **31**, 1671 (1985); D. J. Bergman, *ibid.* **31**, 1696 (1985); M. Sahimi, J. Phys. C **19**, L79 (1986); S. Roux, J. Phys. A **19**, L351 (1986).
 [5] J. G. Zabolitzky, D. J. Bergman, and D. Stauffer, J. Stat. Phys. **44**, 211 (1986).
 [6] S. Arbabi and M. Sahimi, Phys. Rev. B **38**, 7173 (1988); M. Sahimi and S. Arbabi, *ibid.* **47**, 703 (1993); M. Sahimi (private communication).
 [7] M. Plischke and B. Joós, Phys. Rev. Lett. **80**, 4907 (1998).
 [8] M. Plischke, D. C. Vernon, B. Joós, and Z. Zhou, Phys. Rev. E **60**, 3129 (1999).
 [9] O. Farago and Y. Kantor, Phys. Rev. Lett. **85**, 2533 (2000); J. Cohen, M.Sc. thesis, Simon Fraser University, 2001 (unpublished).
 [10] O. Farago and Y. Kantor, Europhys. Lett. **57**, 458 (2002).
 [11] M. Plischke, Phys. Rev. E **73**, 061406 (2006).
 [12] X. Xing, S. Mukhopadhyay, and P. M. Goldbart, Phys. Rev. Lett. **93**, 225701 (2004).
 [13] M. P. Allen and D. J. Tildesley, *Computer Simulation of Liquids* (Oxford University Press, New York, 1987).
 [14] To obtain an estimate of the relaxation times of these systems, I have calculated the stress-stress correlation function $\langle \sigma_{xy}(t)\sigma_{xy}(0) \rangle - \langle \sigma_{xy} \rangle^2$ for a range of p and different system sizes. In equilibrated systems this function has a decay constant of 50–100 time steps for all values of the parameters in both the sheared and unsheared states. I am therefore confident that the systems studied are fully equilibrated.
 [15] M. Tokita and K. Hikichi, Phys. Rev. A **35**, 4329 (1987); M. Djabourov, J. Leblond, and P. Papon, J. Phys. (Paris) **49**, 333 (1988); F. Devreux, J. P. Boilot, F. Chaput, L. Malier, and M. A. V. Axelos, Phys. Rev. E **47**, 2689 (1993); G. C. Fadda, D. Lairez, and J. Pelta, Phys. Rev. E **63**, 061405 (2001).
 [16] C. P. Lusignan, T. H. Mourey, J. C. Wilson, and R. H. Colby, Phys. Rev. E **52**, 6271 (1995).
 [17] M. Daoud and A. Coniglio, J. Phys. A **14**, L30 (1981).
 [18] E. Del Gado, L. de Arcangelis, and A. Coniglio, Phys. Rev. E **65**, 041803 (2002) and references therein.